universe

MDPI

Review

The Complex Upper HR Diagram—Redux: The Low-Metallicity Galaxies

Roberta M. Humphreys

Minnesota Institute for Astrophysics, University of Minnesota, 116 Church St. SE, Minneapolis, MN 55455, USA; roberta@umn.edu

Abstract

The properties of luminous evolved stars in nearby resolved galaxies are briefly reviewed with emphasis on recent results for the low-metallicity dwarf irregulars. Highlights and recent discoveries of some of the more extreme examples with high rates of mass loss such as the yellow and red hypergiants, LBVs, and giant eruptions are summarized. Some of the most interesting new results are the evidence for high-luminosity stars at high redshift and at very low metallicities with mass loss. The presence of an empirical upper luminosity limit at very low metallicities similar to what we observe in the Milky Way and Local Group galaxies is presented. Its implications for the first stars in the early Universe and mass loss mechanisms at very low metallicity are discussed.

Keywords: massive stars; supergiants; hypergiants; HR diagram; H-D limit

1. The Most Luminous, Most Massive Stars

The most luminous stars are also the most massive. Their importance as the progenitors of supernovae and their enrichment of the interstellar medium has been repeated and discussed numerous times and likewise in the papers in this Special Issue. With their intrinsic high luminosities, they are also the first probes of the stellar content of other galaxies. Massive stars are not only important and interesting. They are *fun*, challenging, and they never fail to surprise us. With their strong winds and mass loss, sometimes dramatic, many show significant changes and activity during a human lifetime, providing clues to their evolution, structure, and short lives.

Massive stars are usually acknowledged as those with initial masses above about 9 $M_{\odot}$, with sufficient mass in their cores to initiate Helium fusion without forming a degenerate core. Their upper mass limit is uncertain, but based on the luminosities of the hottest, most luminous O-type stars, it is probably about 200 to 300 $M_{\odot}$ [1]. They range in luminosity from approximately 10^4 up to about 5×10^6 $L_{\odot}$, although there may be a few somewhat above this limit. Figure 1 shows a schematic luminosity-versus-temperature Hertzsprung–Russell Diagram (HR Diagram or HRD) with the locations of different recognized evolutionary groups from 1 to more than 60 $M_{\odot}$. The luminous or massive stars are those above 10^4 and include the super- and hypergiants of different temperatures and the OB and Wolf-Rayet stars outlined on this HRD.

Check for updates

Academic Editor: Vikram Dwarkadas

Received: 1 May 2026
Revised: 20 July 2026
Accepted: 23 July 2026
Published: 31 July 2026

Copyright: © 2026 by the author. Licensee MDPI, Basel, Switzerland. This article is an open access article distributed under the terms and conditions of the Creative Commons Attribution (CC BY) license.

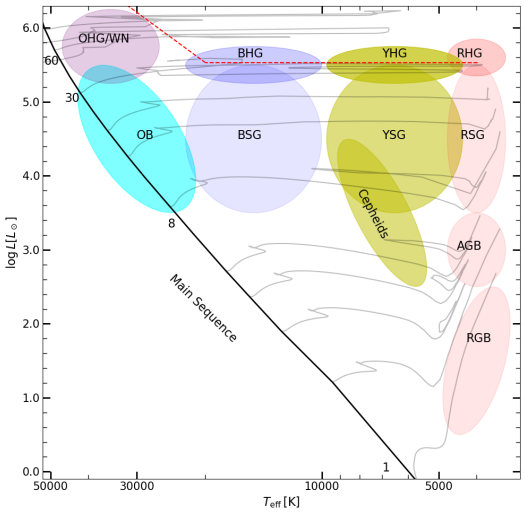


Figure 1. A schematic HR Diagram for populations of evolved stars. Published with permission from Patrick [2]. Massive stars are those above 10^4 $L_{\odot}$. The locations of the red, yellow and blue hypergiants and supergiants and the evolved OB and WN stars are identified. The dashed red line show the location of the Humphreys-Davidson Limit.

2. Massive Stars on the Hertzsprung–Russell Diagram

Distance is the most important parameter for any star or group of stars. Many other stellar parameters, not just luminosity, depend on it, including derived parameters such as size and mass; its placement on the HR Diagram, estimates of its evolutionary state, and comparison with other stars including stellar populations in other galaxies. Distance is the foremost advantage in studying massive stars in nearby galaxies. All the stars are at the same distance. In the Milky Way, similar studies were limited to within a few kpc of the Sun due to a lack of good distances and extinction by dust. This has changed dramatically with parallaxes from the Gaia satellite, but surveys at large distances are incomplete, and the corrections for interstellar extinction are uncertain.

The intrinsically most luminous stars are not only the most massive but also the hottest, while the visually brightest are massive stars of intermediate temperature. Thus, studies of the most luminous stars, their evolution and populations in the Milky Way and nearby resolved galaxies require spectra and multiwavelength observations to estimate their temperatures and determine their bolometric or total luminosities and thus place them on a Hertzsprung–Russell Diagram.

Feast, Thackeray and Wesselink [3] published one of the first HR Diagrams for a massive star population: the brightest stars in the Large and Small Magellanic Clouds. Their HR Diagram, shown in Figure 2, relied on the derived absolute visual magnitudes from membership in the Clouds and spectral types from the HD Catalogs. It did not include the red supergiants and only a few known O-type stars, the hottest stars. The visually most luminous stars with A-type spectra were extraordinarily luminous, with M_{Bol}'s near -10 mag, a result confirmed by many more recent surveys. A recent HRD for the LMC is also shown in Figure 2 for comparison, with bolometric luminosities and effective temperatures for the individual stars based on spectral classification and current calibrations.

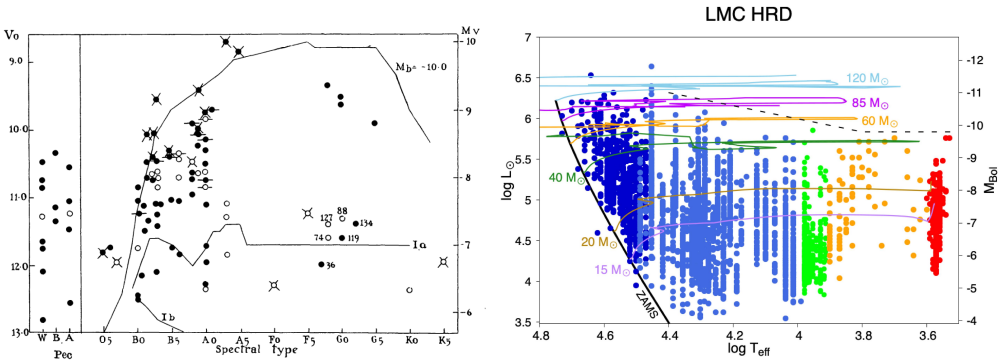


Figure 2. Left: The HR Diagram for the brightest stars in the LMC and SMC from Feast, Thackeray and Wesselink [3]. LMC stars are closed symbols and those in the SMC are shown as open symbols. **Right**: A current HRD for the most luminous stars in the LMC based on their spectral types [4].

With more complete surveys for the OB stars and observations of the red supergiants in the LMC, and in the Milky Way for the supergiants in clusters and associations, a comparison by Humphreys and Davidson [5] revealed comparable populations of massive stars across the HR Diagram and a common upper luminosity boundary or upper limit for the massive stars in both galaxies. They describe the upper luminosity boundary as an envelope of declining luminosity with decreasing temperature for the hottest stars with a constant upper luminosity boundary near $M_{Bol} = -9.5$ mag or $\approx 5.7 \log L/L_{\odot}$ for the cooler, more evolved massive stars, the yellow and red supergiants. This empirical luminosity boundary was not predicted by any models or theory at that time and has important implications for the evolution of the most massive stars. The lack of cool counterparts showed that stars initially above about 40 or 50 $M_{\odot}$ did not evolve to the red supergiant stage. The sloping upper boundary for the hottest stars showed that it was mass-dependent, an important early clue that the upper limit is due to mass loss, limiting evolution to cooler temperatures.

The empirical upper luminosity boundary is confirmed in several nearby resolved galaxies and is now commonly referenced as the Humphreys–Davidson Limit or simply H-D Limit. It has played a major role in our understanding of the role of mass loss, high mass loss events, and the instabilities in evolved massive stars. See Humphreys and Davidson [6] for a recent review of the upper HRD, mass loss, and the mass loss mechanisms that explain the upper limit.

Different types of hot and evolved stars exhibit high mass loss and its effects on their observed characteristics and their evolution. The edited book *Very Massive Stars in the Local Universe* [7] emphasized the importance of the hottest, most luminous stars with reviews of the "very massive stars" (VMS), while *Luminous Stars in Nearby Galaxies* [8] included contributed chapters on giant eruptions, the yellow and red hypergiants, the S Dor/Luminous Blue Variables, Wolf-Rayet stars and others. The introductory chapter [9] is a review of the upper HRD and the massive star populations in nearby galaxies. The next sections in this paper bring those topics up to date, including new results for low-metallicity galaxies. A very recent review of Wolf–Rayet stars [10] can be found in the new *Encyclopedia of Astrophysics*. Examples of some of these evolved post-main-sequence high-mass-loss stars are discussed in the next section.

With larger telescopes and space-based instruments, we can now compare and study massive stars in different galaxies and environments. The VLT Flame spectroscopic survey of the 30 Doradus region (Tarantula Nebula) of the LMC [11,12] has greatly expanded our census of the very most massive, hottest stars. This includes the very crowded R136 complex. Many of the stars are binaries, even multiple systems, and even with the resolution of HST, they are blended. They include high-luminosity O-type stars and WR stars. Due

to crowding and blending in the giant H II regions in more distant Local Group galaxies, however, these stars are not well-represented and are even missing in the available studies. In Section 4, this review is focuses on the similarities and differences of the massive populations in nearby galaxies; thus, these early O stars are not included.

The most massive stars are often considered to be the first stars formed in the Universe, even before the first recognizable galaxies. In the last section, I discussed recent results for the evidence of massive stars at high redshifts and low metallicity and in what ways these populations may be similar to the massive stars we observe now.

3. Some Special Stars

Some stars often appear to have extreme characteristics or behavior, such as variability, exceptional luminosity and mass loss, or a distinctive appearance. They stand out with respect to the majority of stars in their locus on the HRD. They might be dismissed as extreme or as an exception. However, their outstanding features often provide important clues to understanding similar process occurring in the more "typical" examples.

3.1. Eta Carinae, P Cygni, and the S Doradus Variables (LBVs)

Eta Car and P Cygni have long been recognized as special stars. Eta Car is famous for its great eruption in the 1840s. P Cygni gave its name to the distinctive emission line profile that is the clue to mass loss and is the prototype for mass loss in massive hot stars.

Books have been written about eta Car [13], one of the most luminous evolved hot stars known. Today, eta Car has an intrinsic luminosity of $10^{6.7}$ $L_{\odot}$. A massive binary, its primary's initial mass is estimated at 150–200 $M_{\odot}$. During its great eruption in the 1840s, it became the second brightest star in the sky with an estimated luminosity of $10^{7.7}$ $L_{\odot}$ at maximum light, an increase by a factor of 10 when it may have ejected ≈20 $M_{\odot}$. The record of that massive eruption is clearly visible in its classic bipolar image. Light echoes from its great eruption, identified in distant nebulosity [14], have revealed cool absorption-line spectra from its expanding dense ejecta.

Much of what we now know about eta Car is due to the extensive observations with HST which covered more than 20 years. Here I give a short summary of the some of the highlights from those observations, beginning with the initial discovery of its brightening, a factor two in one year, from UV spectra with HST/STIS [15]. The light curve of the central star from HST imaging and spectroscopy covering more than 20 years are shown in Figure 3 with measurements at four different wavelengths from the near-UV, F240W and F330W, and visual and red continua. The very visible dips in the light curve are known as spectroscopic events that occur every 5.54 yrs at periastron when its ≈ 40 $M_{\odot}$ secondary enters the dense wind of the primary. The high excitation emission lines of He I, Fe II and Ne III that dominate its spectrum weaken and even disappear. The spectroscopic events have been showing progressive changes suggesting that the density of the primary's wind has been decreasing [16] due to a decrease in its mass loss rate resulting in reduced dust formation and its very obvious brightening even in ground-based observations. These changes were very apparent in its 2014.6 event compared with previous ones observed with HST/STIS [17].

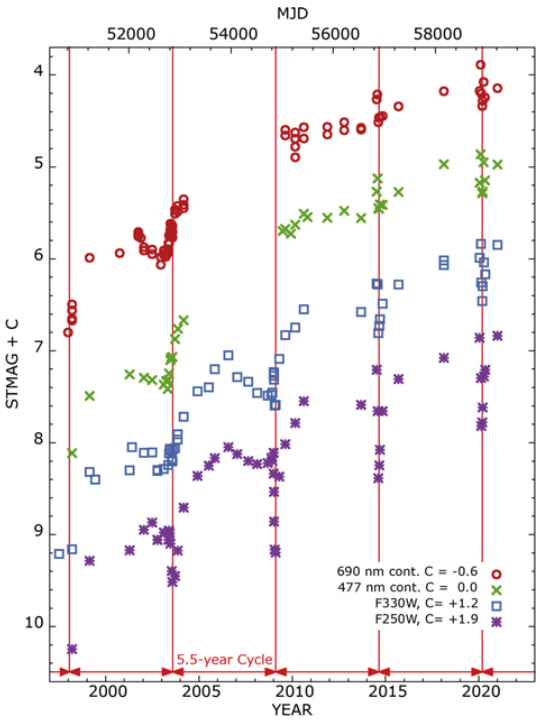


Figure 3. The light curve of eta Car, the central star, from HST imaging and spectroscopy from HST/STIS, illustrating its increasing pparent brightness from the near-UV to to the visible and red wavelengths [18]. The dips every 5.5 years are the "spectroscopic events".

P Cygni is less luminous and less massive than eta Car and at its temperature and luminosity, it may be considered more typical of evolved hot, massive stars. Its historical light curve [19] shows two eruptions in the 17th century when it increased by about three magnitudes in apparent visual brightness, corresponding to a factor of about six in actual luminosity. P Cyg has been slowly increasing in visual brightness since then. Imaging has revealed clouds of gas associated with P Cyg, which are a record of its earlier high-mass-loss events [20,21].

Eta Car and P Cyg have been called Luminous Blue Variables (LBVs) in the literature. In our 1994 review [22], we called them giant eruption LBVs to distinguish them from the S Doradus variables. Both eta Car and P Cyg increased their total luminosity during their eruptions, while the S Dor/LBVs do not show a significant increase in luminosity during their enhanced mass-loss episodes. Eta Car is now recognized as the progenitor or representative of a class of non-terminal giant eruptions, sometimes called SNs impostors [23], discovered in the numerous supernova surveys. Their relation to the LBVs is not established, but what we observe and the energies involved are definitely different.

The S Dor/LBVs are recognized by their characteristic spectroscopic and photometric variability. During their normal "quiescent" state, they are massive hot stars with stellar winds and mass loss typical of their temperatures and luminosities. Due to enhanced mass loss, they increase in visual brightness, and their spectra transition to a cooler state resembling a high-luminosity late A- or F-type supergiant at their visual maximum. We are actually observing a shift in the bolometric correction due to the formation of an optically thick, cooler dense wind or expanded photosphere. See the review by Weis & Bomans [24]. During their quiescent state, the LBVs lie along a common locus in the HRD known as the S Dor instability strip [25]. Figure 4 shows a schematic HRD for the LMC LBVs with the instability strip, illustrating their apparent transits on the HRD in their high-mass-loss state.

There are eight confirmed and six candidate LBVs in the LMC and numerous ones in M31 and M33, plus confirmed examples in the spirals M101, NGC 2403, and M81. In contrast, there is only one confirmed LBV/S Dor variable in the SMC (R40). Notably, the

SMC has significantly lower metallicity than these galaxies, see Table 1. Weis & Bomans [24] discussed the evidence for LBVs in low-metallicity galaxies, specifically the low-metallicity dwarf irregulars, and noted the lack of confimed LBVs in these systems. The dwarf irregular IC 1613 also in the Local Group has one LBV. The peculiar V1 in NGC 2366 [26] is often cited as an example, but it became bluer during its eruption, not redder as in S Dor variability. It may be a giant eruption, more like the historic eruption of P Cyg. This may be more than a metallicity effect and may reflect the smaller sample of evolved massive progenitors, similar to the luminosities of the brightest blue supergiants discussed in Section 4.

Some authors [27] have suggested that LBVs are binaries that have gained mass from binary interaction and are isolated from similar massive stars. However, the large mass range for the LBVs in the instability strip cannot be explained by binarity. Instead, the stars in the strip share a high value of Γ, the Eddington parameter [28]. Furthermore, a recent comprehensive survey and discussion of the spatial distributions of the evolved massive stars in the LMC [29] showed that the LBVs are not isolated from related populations of massive stars.

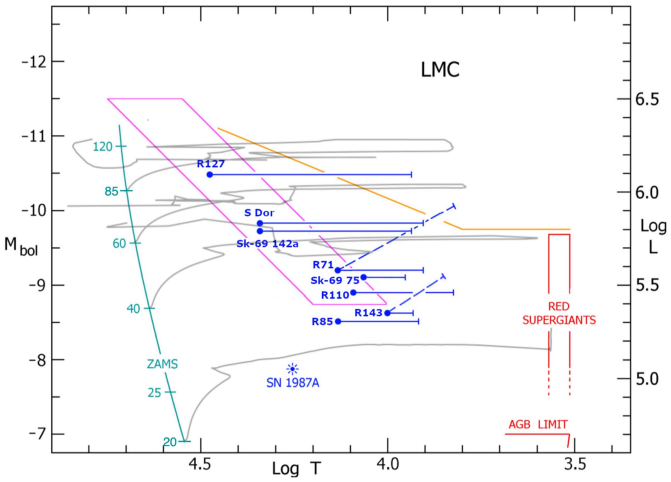


Figure 4. HR Diagram for the confirmed S Dor/LBVs in the LMC [29].

3.2. The Yellow Hypergiants

The intermediate temperature, high-luminosity yellow supergiants or hypergiants and similar red supergiants define the constant-luminosity portion of the upper luminosity boundary, which is cooler than about 10,000 K degrees. These stars have high mass-loss rates. Several have extended circumstellar ejecta, and they make transits in the HR Diagram due to apparent changes in spectral type or temperature attributed to changes in mass loss and their stellar winds. IRC +10420, with its complex circumstellar ejecta and high-mass-loss events, is the prototype of the class. A recent survey of yellow supergiants in the Milky Way [30] shows their distribution on the HR Diagram (Figure 5), with the most luminous just below the H-D limit. In a recent review Jones [31] discusses several examples, their evolutionary state as possible post-red supergiants, and the mass-loss mechanism.

Two stars deserve special mention: Var A in M33 and WOH-G64 in the LMC. Var A is especially significant because it has been observed to transit from an initial yellow supergiant state [32] to an apparent M-type supergiant based on its spectrum, with a rapid decline in brightness and the formation of dust [33]. It then returned to its probable true evolutionary state as a yellow hypergiant in about forty years [34]. These transits on the HRD are best understood as a high-mass-loss episode forming a cooler dense wind which, with respect to the yellow supergiant, resembles a red supergiant. After several decades, the mass loss decreased, the density of the wind decreased, and the underlying

warmer supergiant became visible. In some ways, this mimics the LBV behavior of the hot supergiants but for a cooler, evolved star in a quiescent or normal state.

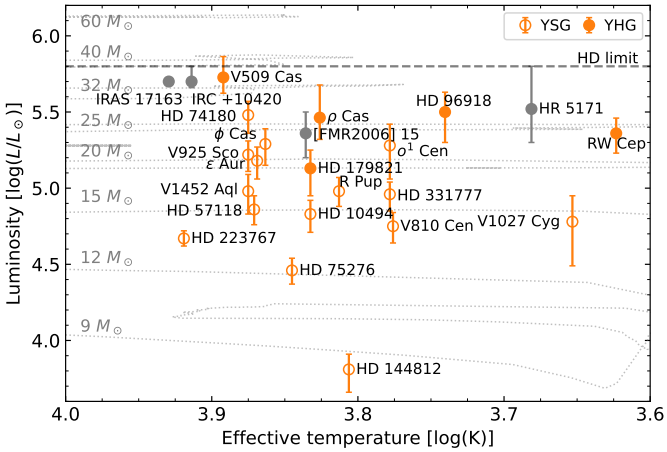


Figure 5. Milky Way yellow supergiants and hypergiants on the HR Diagram. The dashed line is the Humphreys–Davidson Limit. Published with permission from Kasikov et al. [30].

A similar event has been observed for WOH-G64 [35], one of the two most luminous RSGs on the current LMC HRD in Figure 2. The RSG WOH-G64 was well known for its high luminosity, circumstellar dust and high mass-loss rate. It apparently transitioned in a relatively short time in the order of a year, 2013–2014, getting bluer and with a corresponding spectroscopic change from a late M- type star with TiO bands to a much warmer spectrum with H emission and emission lines of CaII and [Ca II] resembling the spectra of the yellow hypergiant IRC +10420 and Var A. The authors consider a possible binary model in which the cool supergiant ejected a pseudo-atmosphere in a common envelope phase or an apparent RSG returned to its quiescent or normal state as a yellow hypergiant, similar to Var A recovering from a high-mass-loss event. Unlike for Var A, we do not have an earlier record of when WOH-G64 was a warmer star.

The TiO bands recently re-appeared in the spectra of WOH-G64 from 2024–2025 described by van Loon and Ohnaka [36], only three years after the most recent spectrum of the yellow hypergiant. The most likely explanation would be that, like other yellow hypergiants, WHO-G64, only recently shedding its dense wind, has had another enhanced mass-loss episode and produced a dense cooler outer envelope or wind with TiO bands. It will be very important to see how long this episode lasts.

3.3. Red Supergiants and Hypergiants—Surface Activity and Mass Loss

There is increasing evidence that red supergiants experience massive directed outflows that result in dimming of the star due to dust formation. The recent "great dimming" of Betelgeuse [37] is probably the best example. UV HST/STIS spectra obtained before the dimming [38,39] show that the star had a gaseous outflow from its chromosphere. As the gas expanded and cooled, it formed dust obscuring part of the image [40]. The historical light curve for the much more luminous RSG, VY CMa, shows an extended period in the early 20th century with at least six "deep minima", each lasting 2–3 years, that correspond with the ejection ages of massive clumps or knots in its circumstellar ejecta [41,42]. The yellow hypergiant RW Cep has also experienced an extended minimum [43,44] and is one of several yellow and red supergiants now known with large-scale surface asymmetries.

The mass estimate of the outflow in Betelgeuse suggests that similar outflows contribute to its total mass lost, while in VY CMa, the more massive clumps dominate its high

mass-loss rate [45]. Thus, surface activity and associated massive ejecta are another source for the mass-loss mechanisms of the red and yellow supergiants.

4. The Local Group and Beyond—The Low-Metallicity Galaxies

The Introductory review chapter [9] in *Luminous Stars in Nearby Galaxies* included a summary of the most luminous stars of different types in local group galaxies and others with resolved stellar populations with a description of the numerous surveys and results from different research groups. Table 1 from [9] is copied here, with additional entries for the LMC [4,46] and NGC 2403 [47]. Since then, additional work, especially on nearby galaxies with low metallicity, has become available and is presented in Table 2. Surveys for the hottest stars are incomplete in these galaxies. The massive hottest stars are in extremely crowded regions with blended images and many are multiple. Consequently, the O-type stars which will be the most luminous and most massive stars in their galaxies are not included. Likewise, OB stars in crowded regions may be missed. The bolometric luminosities for the three most luminous stars are listed for each spectral type group. The adopted distances for all the galaxies is based on the Cepheid scale, except for TRGB for IC 10. References for the adopted distance moduli and the entries in Tables 1 and 2 are in the footnotes.

Entries for the yellow supergiants (FGKs) are lacking for several galaxies. They are undoubtedly present, but surveys for the blue or hot supergiants and likewise for the red supergiants may miss these intermediate-temperature stars, which also overlap with foreground stars. Data for the blue supergiants in the highly-obscured starburst galaxy IC 10 is missing. Several papers on X-ray binaries in IC 10 mention blue supergiants, but no photomery or spectra of individual stars is reported.

Two important trends are apparent for the luminosities for the blue and red supergiants in these two tables. The well-known dependence of the brightest "blue" supergiants, the high-luminosity A-type stars, on the luminosity of the parent galaxy is reinforced with the dwarf irregular galaxies in Table 2. Admittedly, differences in the adopted distance moduli and corrections for interstellar extinction could result in differences of 0.1 to 0.2 mag in the derived luminosities, but the trend appears to be real. This is not a metallicity effect. NGC 6822, for example, has a metallicity comparable to NGC 300 and NGC 55, but less luminous A-type supergiants and a significantly lower galactic luminosity. It is most likely a size of sample effect. The more luminous, more massive galaxies will have a larger progenitor population of massive stars, and therefore at any given time will have more of the most luminous evolved stars. The trend is most obvious for WLM. The two large Sb-type spirals, M31 and M81, appear to be the exception, but they have lower star formation rates, not lower masses, than the Sc spirals, and comparable metallicities.

Two phenomena may be occurring with the red and yellow supergiants. The constant upper luminosity boundary for the evolved supergiants is defined by the red and yellow supergiants [5,6]. In the original papers for the Milky Way and LMC, this was at ≈ -9.5 M_{Bol}. Considerable work has been done since then, including refinement of the Cepheid distance scale. Nevertheless, this upper limit is approximately the same for the YSGs and RSGs in the six Sb and Sc spirals in Table 1. Note that confirming spectroscopy for RSG candidates in NGC 2403 is incomplete. However, the upper luminosities for the red and yellow supergiants are noticeably lower in the less luminous, lower-metallicity galaxies in both tables, with $M_{Bol} \approx -9.2$ for the SMC and -8.8 to -8.6 for WLM and IC 10. To a first order, this is most likely the consequnce of the lower luminosities for the most luminous A-type supergiants, their immediate predecessors.

Table 1. The Most luminous stars (M_{Bol}) of different spectral types.

Galaxy	**M31** [1]	**M33** [1]	**LMC** [2]	**SMC** [2]	**NGC 6822** [3]	**IC 1613** [3]	**NGC 2403** [4]	**M81** [4]	**M101** [4]
Type	**Sb I-II**	**Sc II**	**Im**	**Im**	**Im**	**Ir**	**Sc III**	**Sb I-II**	**Sc I**
M_v	**−21.5**	**−18.9**	**−18.5**	**−16.8**	**−15.2**	**−14.8**	**−19.3**	**−20.9**	**−21.0**
$Z/Z_\odot$	**1.5**	**0.5-0.3**	**0.5**	**0.2**	**0.3**	**0.2**	**0.8-0.5**	**0.9**	**1-0.4**
Spectral Type	M_{Bol}	M_{Bol}	M_{Bol}	M_{Bol}	M_{Bol}	M_{Bol}	M_{Bol}	M_{Bol}	M_{Bol}
O9.5 – B5	−10.6 (2)	−10.1	−10.9	−10.3 (2)	−10.3	−9.5	−10.0 (2)	−10.6	...
	−10.2	−10.0	−10.7	−10.2	−9.9	−8.8	−9.5	−10.0	...
	−10.0 (2)	−9.8	−10.0	−9.8 (2)	−9.5	−8.7	−9.4	−9.7	...
B8 – A8	−9.3	−10.1 (B324)	−9.6 (HD33579)	−9.6 (HD7583)	−8.1	−8.4	−9.8	−9.3	−10.4 (2)
	−9.1	−9.5 (2)	−9.0	−9.2	−7.7	−6.9	−9.5	−9.1 (2)	−10.3
	−8.9 (2)	−9.4	−8.9	−9.0	−7.5	−6.7	−9.4	−8.9	−9.9
FGK	−9.8	−9.6 (2)	−9.6	−9.2	...	...	−9.5	−9.7	−9.8
	−9.7	−9.5 (Var A)	−9.5 (3)	−9.1	...	...	−9.3	−9.6	−9.3
	−9.5	−9.2 (3)	−9.2 (3)	−8.1	...	...	−8.8	−9.4	−9.2
RSGs	−9.4 (2)	−9.6	−9.6 (WOH-G64)	−9.2	−9.2	−9.4	−8.5	−9.5:	−9.9:
	−9.3	−9.5 (2)	−9.6	−9.1	−9.1	−8.8	−8.4 (2)	−9.2 (2)	−9.5
	−9.1 (2)	−9.4 (2)	−8.9 (2)	−8.9	−8.7	−8.7	...	...	−9.2

[1] **M31 and M33**; M31 DM 24.4 [48], M33 DM 24.5 [49], BSGs and RSGs [50–59]. [2] **LMC and SMC**; LMC DM 18.5, SMC DM 18.9, RSGs [60–63]. [3] **NGC 6822 and IC 1613**; N6822 DM 23.4 [64], IC 1613 DM 24.3 [65], BSGs and RSGs [66–69]. [4] **NGC 2403, M81 and M101**; N2403 DM 27.5, M81 DM 27.8, M101 29.1 [70], BSGs and RSGs [71–73].

Table 2. The most luminous stars (M_{Bol}) of different spectral types (Part 2).

Galaxy	**NGC 300** [1]	**NGC 55** [2]	**IC 10** [3]	**WLM** [4]
Type	**Scd**	**Im(B)**	**dIr(B)**	**dIr**
M_v	**−17.4**	**−18.5**	**...**	**−14.0**
$Z/Z_\odot$	**0.4**	**0.3**	**0.3**	**0.1**
Spectral Type	M_{Bol}	M_{Bol}	M_{Bol}	M_{Bol}
O9.5 – B5	−10 (WN11)	−10.1	...	−9.5
	−9.7	−9.4	...	−8.7
	−9.5 (2)	−9.3	...	−8.6
B8 – A8	−9.2	−9.0 (2)	...	−7.4
	−9.1	−8.3	...	−7.1
	−8.6	−7.9 (2)	...	−6.8
FGK	...	−8.2	−8.5	−8.5
	...	...	...	−6.8
	...	...	...	...
RSGs	−9.3	−8.6	−8.6	−8.8
	−9.0	−8.3	−8.4 (2)	−7.7
	−8.8 (2)	−8.1 (2)	...	−7.6

[1] **NGC 300**; DM 26.4 [74], BSGs [75,76], RSGs [77,78]. [2] **NGC 55**; DM 26.4 [79], BSGs [80], RSGs [78]. [3] **IC 10**; DM 24.4 [81], RSGs [82]. [4] **WLM**; DM 25.0 [83,84], BSGs [85], RSGs [78,82,86].

The red supergiants also exhibit a consequence of lower metallicity on their spectral classifications, with a shift in apparent spectral types from types M to K-type spectra. This was first noticed for the red supergiants in the SMC by [87] and confirmed in later, fainter surveys [88,89]. It is attributed to the lower metallicity in the SMC and the corresponding reduced opacity. We see the same shift in the lower-metallicity galaxies in Table 2. Indeed, in WLM, there are two early K-type, two K5 I, and one M 1-3 type classifications for the red supergiants [86]. In Table 2, the K5 stars are listed as RSGs. This shift to a warmer temperatures with a lower bolometric correction would also contribute to a lower upper luminosity limit for the YSGs and RSGs.

5. Massive Stars at High z and Low Z

Recent papers on gravitational lensing have identified potentially massive stars in distant galaxies at high redshift [90]. These studies have revealed information about the massive star populations in the lensed galaxies at high z. The H-D limit has been used to set limits on the predicted population and for comparison with different models for the stars at high redshift. For example, the H-D limit has been used to imply limits on the temperatures of the lensed stars [91] and the radii of black holes in mergers in lensed systems [92]. In a series of papers [93–95] on the supergiant populations in lensed galaxies, the authors conclude that their results are "consistent with a scenario where the H-D limit is also valid at z = 1" [95]. The H-D limit is due to mass loss, specifically high-mass-loss episodes in evolved stars above about 50 $M_\odot$. Thus, mass loss may be important for understanding the evolution of stars in the early univers, but these stars are expected to be of very low metallicity, and this of course brings into question mass loss at low metallicity.

Schootmeijer et al. [96] have identified a constant upper luminosity boundary at $\log L \approx 5.6\ L_\odot$ ($M_{Bol} - 9.25$) for the red supergiants in low-metallicity galaxies and specifically for the very-low-metallicity I Zw 18 with 1/40th $Z_\odot$. Its color–magnitude diagrams for the near-infrared and visual are shown in Figure 6. This upper limit is comparable to the upper luminosities of the red and yellow supergiants in the lower metallicity galaxies in the above tables. The same shift to apparent warmer temperatures is also visible in the

RSGs in I Zw 18. The M-type supergiants typically have intinsic V-I colors greater than 2.0 mag. Although spectra are not available, the reddest stars in the CMD have $(V\text{-}I)_0$ colors of about 1.5 mag. Thus the same blueward shift due to low metallicity is observed. In addition, I Zw 18 is a starburst galaxy with a population of Wolf-Rayet stars, with WN and WC types, due to the loss of their Hydrogen envelopes. The authors conclude that metallicity–independent mass loss is the most likely explanation for the upper luminosity limit in I Zw 18 and the presence of the WR stars. I Zw 18's HRD has a lack of evolved stars above the upper luminosity boundary for the cool stars and also a lack of more massive stars cooler than the WR stars. Thus the H-D limit is present at very low metallicity. This of courses raises questions about mass loss mechanisms effective at low Z.

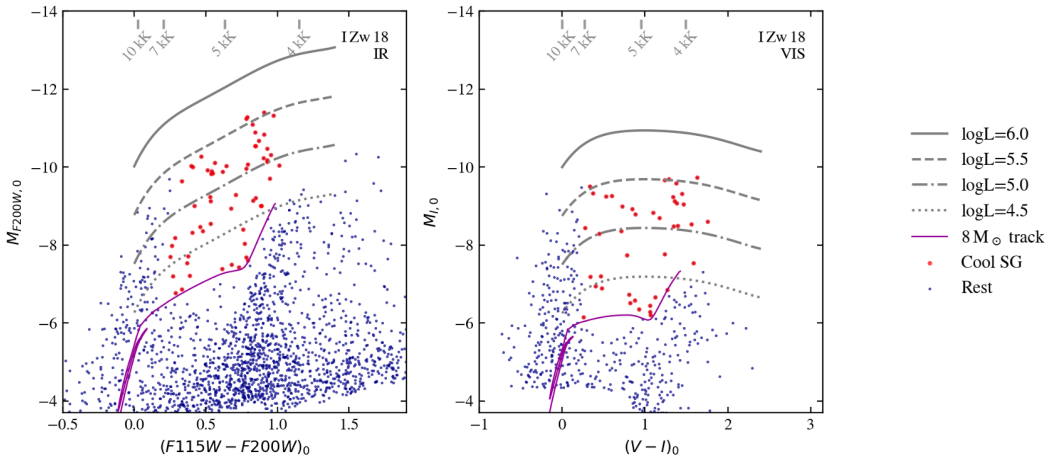


Figure 6. The CMDs for I Zw 18. The candidate RSGs and YSGs are shown in red. The curved lines are the expected loci of constant luminosity from 10^4 to 10^6 $L_\odot$. The red curve is the evolutionary track for a low-metallicity 8 $M_\odot$ star. Published with permission from Schootemeijer et al. [96].

As we emphasized in [6], evolved massive stars close to their Eddington Limit, at Γ = 0.6–0.8, will be unstable to hydrodynamical effects such as turbulence and strange mode instabilities [97,98] leading to high-mass-loss episodes and limiting their evolution to cooler temperatures. The standard metallicity-dependent mass-loss processes operating in the Milky Way and galaxies of the Local Group will not be effective in bringing these very-low-metallicity stars in proximity to their Eddington Limit. Processes that may lead to mass loss at low metallicity include the increasing opacity of Hydrogen as the star expands and cools, rotation, pulsation, of course turbulence and convection, and the strange mode instabilities. The possible roles of magnetic fields and surface activity have not been investigated. See the review by Davidson [99] on radiation-driven stellar eruptions for a discussion of the application and limits of mass loss mechanisms.

6. Remaining Questions

The basic outline of massive star evolution is well understood. Mass loss and its impact on stellar evolution is observed, although details in many cases are still "to be determined". Binaries and binary mergers and interactions are a current hot topic, but many stars in binary systems will evolve as single stars. The origins of the non-terminal giant eruptions in the SN impostors is an outstanding theoretical problem. Possible post-red supergiant evolution and the progenitors of different types of supernovae questions as well regarding which stars become neutron stars and black holes. With the probability of mass loss at very low metallicity and its impact on the first stars and the early Universe, there are many new questions. Massive stars never cease to surprise. Their diversity and activity is what makes them *fun*.

Funding: This research received no external funding.

Data Availability Statement: The data referenced here is available in the published papers and at SIMBAD.

Conflicts of Interest: The author declares no conflicts of interest.

Abbreviations

The following abbreviations are used in this manuscript:

HRD	Hertzsprung–Russell Diagram
H-D Limit	Humphreys–Davidson Limit
RSG	Red Supergiant
YSG	Yellow Supergiant

References

1. Bestenlehner, J.M.; Crowther, P.A.; Caballero-Nieves, S.M.; Schneider, F.R.N.; Simon-Diaz, S.; Brands, S.A.; de Koter, A.; Gräfener, G.; Herrero, A.; Laner, N.; et al. The R136 star cluster dissected with Hubble Space Telescope/STIS-II. Physical properties of the most massive stars in R136. *Mon. Not. R. Astron. Soc.* **2020**, *499*, 1918–1936. [CrossRef]
2. Patrick, L.R. Giants, supergiants, and hypergiants. *Encycl. Astrophys.* **2026**, *2*, 470–487. [CrossRef]
3. Feast, M.W.; Thackeray, A.D.; Wesselink, A.J. The Brightest Stars in the Magellanic Clouds. *Mon. Not. R. Astron. Soc.* **1960**, *121*, 337–385. [CrossRef]
4. Martin, J.C.; Humphreys, R.M. A Census of the Most Luminous Stars. I. The Upper HR Diagram for the Large Magellanic Cloud. *Astron. J.* **2023**, *166*, 214–225. [CrossRef]
5. Humphreys, R.M.; Davidson, K. Studies of luminous stars in nearby galaxies. III-Comments on the evolution of the most massive stars in the Milky Way and the Large Magellanic Cloud. *Astrophys. J.* **1979**, *232*, 409–420. [CrossRef]
6. Humphreys, R.M.; Davidson, K. Reflections on the Upper Hertzsprung-Russell Diagram. *Astrophys. Sp. Sci.* **2025**, *370*, 100. [CrossRef]
7. Vink, J.S. (Ed.) *Very Massive Stars in the Local Universe*; Astrophysics and Space Science Library; Springer: New York, NY, USA, 2015; Volume 412. [CrossRef]
8. Humphreys, R.M. (Ed.) *Luminous Stars in Nearby Galaxies*; MDPI: Basel, Switzerland, 2020.
9. Humphreys, R.M. The Complex Upper HR Diagram. *Galaxies* **2020**, *7*, 75. [CrossRef]
10. Shenar, T. Wolf-Rayet Stars. *Encycl. Astrophys.* **2026**, *2*, 569–583. [CrossRef]
11. Evans, C.J.; Taylor, W.D.; Hénault-Brunet, V.; Sana, H.; de Koter, A.; Simón-Díaz, S.; Carraro, G.; Bagnoli, T.; Bastian, N.; Bestenlehner, J.M.; et al. The VLT-FLAMES Tarantula Survey. I. Introduction and observational overview. *Astron. Astrophys.* **2011**, *530*, 108–161. [CrossRef]
12. Crowther, P.A. Massive Stars in the Tarantula Nebula: A Rosetta Stone for Extragalactic Supergiant HII Regions. *Galaxies* **2019**, *7*, 88. [CrossRef]
13. Davidson, K.; Humphreys, R.M. (Eds.) *Eta Carina and the Supernova Impostors*; Astrophysics and Space Science Library; Springer: New York, NY, USA, 2012; Volume 384. [CrossRef]
14. Rest, A.; Prieto, J.L.; Walborn, N.R.; Smith, N.; Bianco, F.B.; Chornock, R.; Welch, D.L.; Howell, D.A.; Huber, M.E.; Foley, R.J.; et al. Light Echoes Reveal an Unexpectedly Cool eta Carinae during its Nineteenth-Century Eruption. *Nature* **2012**, *482*, 375–378. [CrossRef]
15. Davidson, K.; Gull, T.R.; Humphreys, R.M.; Ishibashi, K.; Whitelock, P.; Berdnikov, L.; McGregor, P.J.; Metcalfe, T.S.; Polomski, E.; Hamuy, M. An Unusual Brightening Of Eta Carinae. *Astron. J.* **1999**, *118*, 1777–1783. [CrossRef] [PubMed]
16. Mehner, A.; Davidson, K.; Humphreys, R.M.; Martin, J.C.; Ishibashi, K.; Ferland, G.; Walborn, N. A Sea Change in Eta Carinae. *Astrophys. J. Lett.* **2010**, *717*, L22–L25. [CrossRef]
17. Mehner, A.; Davidson, K.; Humphreys, R.M.; Martin, J.C.; Ishibashi, K.; Ferland, G.J.; Walborn, N.R. Eta Carinae's 2014.6 spectroscopic event: Clues to the long-term recovery from its Great Eruption. *Astron. Astrophys.* **2015**, *578*, 122–141. [CrossRef]
18. Martin, J.C.; Davidson, K.; Humphreys, R.M.; Ishibashi, K. The Altered State of eta Carinae: HST's Photometric Record 1998–2021. *Res. Notes AAS* **2021**, *5*, 197–201. [CrossRef]
19. de Groot, M. The most luminous stars in the universe. *Ir. Astron. J.* **1988**, **18**, 163–170.
20. Barlow, M.J.; Drew, J.E.; Meaburn, J.; Massey, R.M. The Shock-Excited P-Cygni Nebula. *Mon. Not. R. Astron. Soc.* **1994**, *268*, L29. [CrossRef]

21. Meaburn, J.; O'COnnor, J.A.; López, J.A.; Bryce, M.; Redman, M.P.; Noriega-Crespo, A. The ejecta from the luminous blue variable star P Cygni. *Mon. Not. R. Astron. Soc.* **2000**, *318*, 561–572. [CrossRef]
22. Humphreys, R.M.; Davidson, K. The Luminous Blue Variables: Astrophysical Gey sers. *Publ. Astron. Soc. Pac.* **1994**, *106*, 1025–1051. [CrossRef] [PubMed]
23. Van Dyk, S.D.; Matheson, T. The Supernova Impostors. In *Eta Carina and the Supernova Impostors*; Davidson, K., Humphreys, R.M., Eds.; Astrophysics and Space Science Library; Springer: New York, NY, USA, 2012; Volume 384, pp. 249–274.
24. Weis, K.; Bomans, D.J. Luminous Blue Variables. *Galaxies* **2020**, *8*, 20. [CrossRef]
25. Wolf, B. Empirical amplitude-luminosity relation of S Doradus variables and extragalactic distances. *Astron. Astrophys.* **1989**, *217*, 87–91.
26. Drissen, L.; Crowther, P.A.; Smith, L.J.; Roberta, C.; Roy, J.R.; Hillier, D.J. Physical Parameters of Erupting Luminous Blue Variables: NGC2363-V1, Caught in the Act. *Astrophys. J.* **2001**, *546*, 484–495. [CrossRef]
27. Smith, N.; Tombleson, R. Luminous blue variables are antisocial: Their isolation implies that they are kicked mass gainers in binary evolution. *Mon. Not. R. Astron. Soc.* **2015**, *447*, 598–617. [CrossRef]
28. Humphreys, R.M.; Weis, K.; Davidson, K.; Gordon, M.S. On the Social Traits of Luminous Blue Variables. *Astrophys. J.* **2016**, *825*, 64–79. [CrossRef]
29. Martin, J.C.; Humphreys, R.M.; Davidson, K. On the Spatial Distribution of Luminous Blue Variables, B[e] Supergiants, and Wolf-Rayet Stars in the Large Magellanic Cloud. *Astrophys. J.* **2025**, *994*, 159–189. [CrossRef]
30. Kasikov, A.; Mehner, A.; Kolka, I.; Aret, A. Painting a Family Portrait of the Yellow Super- and Hypergiants in the Milky Way I. Constraining the Distances and Luminosities. *arXiv* **2026**, arXiv:2602.02449. [CrossRef]
31. Jones, T.J. Red and Yellow Hypergiants. *Galaxies* **2025**, *13*, 43. [CrossRef]
32. Hubble, E.; Sandage, A. The Brightest Variable Stars in Extragalactic Nebulae. I. M31 and M33. *Astrophys. J.* **1953**, *118*, 353–361. [CrossRef] [PubMed]
33. Humphreys, R.M.; Jones, T.J.; Gehrz, R.D. The Enigmatic Object Variable A in M33. *Astron. J.* **1987**, *94*, 315. [CrossRef] [PubMed]
34. Humphreys, R.M.; Jones, T.J.; Polomski, E.; Koppelman, M.; Helton, A.; McQuinn, K.; Gehrz, R.D.; Woodward, C.E.; Wagner, R.M.; Gordon, K.; et al. M33's Variable A: A Hypergiant Star More Than 35 YEARS in Eruption. *Astron. J.* **2006**, *131*, 2105. [CrossRef] [PubMed]
35. Muñoz-Sanchez, G.; Kalitsounaki, M.; de Wit, S.; Antoniadis, K.; Bonanos, A.Z.; Zapartas, E.; Boutsia, K.; Christodoulou, E.; Maravelias, G.; Soszyński, I.; et al. The dramatic transition of the extreme Red Supergiant WOH G64 to a Yellow Hypergiant. *Nat. Astron.* **2025**, *10*, 702–713. [CrossRef]
36. van Loon, J.T.; Ohnaka, K. A phoenix rises from the ashes: WOH G64 is still a red supergiant, for now. *Mon. Not. R. Astron. Soc.* **2026**, *546*, 1–6. [CrossRef]
37. Guinan, E.F.; Wasatonic, R.J.; Calderwood, T.J. The Fainting of the Nearby Red Supergiant Betelgeuse. *Astron. Telegr.* **2019**, 13341.
38. Dupree, A.K.; Strassmeier, K.G.; Matthews, L.D.; Uitenbroek, H.; Calderwood, T.; Granzer, T.; Guinan, E.F.; Leike, R.; Montargès, M.; Richards, A.M.S.; et al. Spatially Resolved Ultraviolet Spectroscopy of the Great Dimming of Betelgeuse. *Astrophys. J.* **2020**, *899*, 68–79. [CrossRef]
39. Dupree, A.K.; Strassmeier, K.G.; Calderwood, T.; Granzer, T.; Weber, M.; Kravchenko, K.; Matthews, L.D.; Montargès, M.; Tappin, J.; Thompson, W.T. The Great Dimming of Betelgeuse: A Surface Mass Ejection and Its Consequences. *Astrophs. J.* **2022**, *936*, 18. [CrossRef]
40. Montargès, M.; Cannon, E.; Lagadec, E.; de Koter, A.; Kervella, P.; Sanchez-Bermudez, J.; Paladini, C.; Cantalloube, F.; Decin, L.; Scicluna, P.; et al. A dusty veil shading Betelgeuse during its Great Dimming. *Nature* **2021**, *594*, 365–368. [CrossRef] [PubMed]
41. Humphreys, R.M.; Davidson, K.; Richards, A.M.S.; Ziurys, L.M.; Jones, T.J.; Ishibashi, K. The Mass- loss History of the Red Hypergiant VY CMa. *Astron. J.* **2021**, *161*, 98–108. [CrossRef]
42. Humphreys, R.M.; Richards, A.M.S.; Davidson, K.; Singh, A.P.; Decin, L.; Ziurys, L.M. The Hidden Clumps in VY CMa Uncovered by ALMA. *Astron. J.* **2024**, *167*, 94–106. [CrossRef]
43. Anugu, N.; Baron, F.; Gies, D.R.; Lanthermann, C.; Schaefer, G.H.; Shepard, K.A.; Brummelaar, T.T.; Monnier, J.D.; Kraus, S.; Le Bouquin, J.-B.; et al. The Great Dimming of the Hypergiant Star RW Cephei: CHARA Array Images and Spectral Analysis. *Astron. J.* **2023**, *166*, 78–89. [CrossRef]
44. Anugu, N.; Gies, D.R.; Roettenbacher, R.M.; Monnier, J.D.; Montargés, M.; Mérand, A.; Baron, F.; Schaefer, G.H.; Shepard, K.A.; Kraus, S.; et al. Time Evolution Images of the Hypergiant RW Cephei during the Rebrightening Phase Following the Great Dimming. *Astrophys. J.* **2024**, *973*, L5–L24. [CrossRef]
45. Humphreys, R.M.; Jones, T.J. Episodic Gaseous Outflows and Mass Loss from Red Supergiants. *Astron. J.* **2022**, *163*, 103–109. [CrossRef]
46. Humphreys, R.M.; Jones, T.J.; Martin, J.C. Yellow Supergiants and Post-red Supergiant Evolution in the Large Magellanic Cloud. *Astron. J.* **2023**, *166*, 50–57. [CrossRef]

47. Bresolin, F.; Kudritzki, R.P.; Urbaneja, M. The Metallicity and Distance of NGC 2403 from Blue Supergiants. *Astrophys. J.* **2022**, *940*, 32–46. [CrossRef]
48. Riess, A.G.; Fliri, J.; Valls-Gabaud, D. Cepheid Period-Luminosity Relations in the Near-infrared and the Distance to M31 from the Hubble Space Telescope Wide Field Camera 3. *Astrophys. J.* **2012**, *745*, 156. [CrossRef]
49. Scowcroft, V.; Bersier, D.; Mould, J.R.; Wood, P.R. The effect of metallicity on Cepheid magnitudes and the distance to M33. *Mon. Not. R. Astron. Soc.* **2009**, *396*, 1287–1296. [CrossRef]
50. Massey, P.; Silva, D.R.; Levesque, E.M.; Plez, B.; Olsen, K.A.G.; Clayton, G.C.; Meynet, G.; Maeder, A. Red Supergiants in the Andromeda Galaxy (M31). *Astrophys. J.* **2009**, *703*, 420–440. [CrossRef]
51. Drout, M.R.; Massey, P.; Meynet, G.; Tokarz, S.; Caldwell, N. Yellow Supergiants in the Andromeda Galaxy (M31). *Astrophys. J.* **2009**, *703*, 441–460. [CrossRef]
52. Drout, M.R.; Massey, P.; Meynet, G. The Yellow and Red Supergiants of M33. *Astrophys. J.* **2012**, *750*, 97. [CrossRef]
53. Humphreys, R.M.; Davidson, K.; Grammer, S.; Kneeland, N.; Martin, J.C.; Weis, K.; Burggraf, B. Luminous and Variable Stars in M31 and M33. I. The Warm Hypergiants and Post-red Supergiant Evolution. *Astrophys. J.* **2013**, *773*, 46. [CrossRef]
54. Humphreys, R.M.; Davidson, K.; Grammer, S.; Kneeland, N.; Martin, J.C.; Weis, K.; Burggraf, B. Luminous and Variable Stars in M31 and M33. II. Luminous Blue Variables, Candidate LBVs, Fe II Emission Line St ars, and Other Supergiants. *Astrophys. J.* **2014**, *790*, 48. [CrossRef]
55. Gordon, M.S.; Humphreys, R.M.; Jones, T.J. Luminous and Variable Stars in M31 and M33. III. The Yellow and Red Supergiants and Post-red Supergiant Evolution. *Astrophys. J.* **2016**, *825*, 50. [CrossRef]
56. Massey, P.; Evans, K.A. The Red Supergiant Content of M31. *Astrophys. J.* **2016**, *826*, 224. [CrossRef]
57. Massey, P.; Neugent, K.F.; Smart, B.M. A Spectroscopic Survey of Massive Stars in M31 and M33. *Astrophys. J.* **2016**, *152*, 62. [CrossRef]
58. Humphreys, R.M.; Davidson, K.; Grammer, S.; Kneeland, N.; Martin, J.C.; Weis, K.; Burggraf, B. Luminous and Variable Stars in M31 and M33. IV. Luminous Blue Variables, Candidate LBVs, B[e] Supergiants, and the Warm Hypergiants: How to Tell Them Apart. *Astrophys. J.* **2017**, *836*, 64. [CrossRef]
59. Humphreys, R.M.; Davidson, K.; Hahn, D.; Martin, J.C.; Weis, K. Luminous and Variable Stars in M31 and M33. V. The Upper HR Diagram. *Astrophys. J.* **2017**, *844*, 40. [CrossRef]
60. Bonanos, A.Z.; Massa, D.L.; Sewilo, M.; Lennon, D.J.; Panagia, N.; Smith, L.J.; Meixner, M.; Babler, B.L.; Bracker, S.; Meade, M.R.; et al. Spitzer SAGE Infrared Photometry of Massive Stars in the Large Magellanic Cloud. *Astron. J.* **2009**, *138*, 1003–1021. [CrossRef]
61. Bonanos, A.Z.; Lennon, D.J.; Köhlinger, F.; van Loon, J.T.; Massa, D.L.; Sewilo, M.; Evans, C.J.; Panagia, N.; Babler, B.L.; Block, M.; et al. Spitzer SAGE-SMC Infrared Photometry of Massive Stars in the Small Magellanic Cloud. *Astron. J.* **2010**, *140*, 416–429. [CrossRef]
62. Neugent, K.F.; Massey, P.; Skiff, B.; Drout, M.R.; Meynet, G.; Olsen, K.A.G. Yellow Supergiants in the Small Magellanic Cloud: Putting Current Evolutionary Theory to the Test. *Astrophys. J.* **2010**, *719*, 1784–1795. [CrossRef]
63. Neugent, K.F.; Massey, P.; Skiff, B.; Meynet, G. Yellow and Red Supergiants in the Large Magellanic Cloud. *Astrophys. J.* **2012**, *749*, 177–189. [CrossRef]
64. Feast, M.W.; Whitelock, P.A.; Menzies, J.W.; Matsunaga, N. The Cepheid distance to the Local Group galaxy NGC 6822. *Mon. Not. R. Astron. Soc.* **2012**, *421*, 2998–3003. [CrossRef]
65. Scowcroft, V.; Freedman, W.L.; Madore, B.F.; Monson, A.J.; Persson, S.E.; Seibert, M.; Rigby, J.R.; Melbourne, J. The Carnegie Hubble Program: The Infrared Leavitt Law in IC 1613. *Astrophys. J.* **2013**, *773*, 106. [CrossRef]
66. Humphreys, R.M. Studies of luminous stars in nearby galaxies. V—The local group irregulars NGC 6822 and IC 1613. *Astrophys. J.* **1980**, *238*, 65–78. [CrossRef]
67. Massey, P.; Armandroff, T.E.; Pyke, R.; Patel, K.; Wilson, C.D. Hot, Luminous Stars in Selected Regions of NGC 6822, M31, and M33. *Astron. J.* **1995**, *110*, 2715–2745. [CrossRef] [PubMed]
68. Massey, P. Evolved Massive Stars in the Local Group. I. Identification of Red Supergiants in NGC 6822, M31, and M33. *Astrophys. J.* **1998**, *501*, 153–174. [CrossRef] [PubMed]
69. Bresolin, F.; Urbaneja, M.A.; Gieren, W.; Pietrzyński, G.; Kudritzki, R. VLT Spectroscopy of Blue Supergiants in IC 1613. *Astrophys. J.* **2007**, *671*, 2028–2039. [CrossRef]
70. Freedman, W.L.; Madore, B.F.; Gibson, B.K.; Ferrarese, L.; Kelson, D.D.; Sakai, S.; Mould, J.R.; Kennicutt, R.C., Jr.; Ford, H.C.; Graham, J.A. Final Results from the Hubble Space Telescope Key Project to Measure the Hubble Constant. *Astrophys. J.* **2001**, *553*, 47–72. [CrossRef] [PubMed]
71. Grammer, S.H.; Humphreys, R.M.; Gerke, J. The Massive Star Population in M101. III. Spectra and Photometry of the Luminous and Variable Stars. *Astron. J.* **2015**, *149*, 152. [CrossRef]
72. Humphreys, R.M.; Stangl, S.; Gordon, M.S.; Davidson, K.; Grammer, S.H. Luminous and Variable Stars in NGC 2403 and M81. *Astron. J.* **2019**, *157*, 22. [CrossRef]

73. Kudritzki, R.; Urbaneja, M.A.; Gazak, Z.; Bresolin, F.; Przybilla, N.; Gieren, W.; Pietrzyński, G. Quantitative Spectroscopy of Blue Supergiant Stars in the Disk of M81: Metallicity, Metallicity Gradient, and Distance. *Astrophys. J.* **2012**, *747*, 15–34. [CrossRef]
74. Gieren, W.; Pietrzyński, G.; Soszyński, I.; Bresolin, F.; Kudritzki, R.; Minniti, D.; Storm, J. The Araucaria Project: Near-Infrared Photometry of Cepheid Variables in the Sculptor Galaxy NGC 300. *Astrophys. J.* **2005**, *628*, 695–703. [CrossRef] [PubMed]
75. Bresolin, F.; Gieren, W.; Kudritzki, R.; Pietrzyński, G.; Przybilla, N. Spectroscopy of Blue Supergiants in the Spiral Galaxy NGC 300. *Astrophys. J.* **2002**, *567*, 277–288. [CrossRef] [PubMed]
76. Kudritzki, R.P.; Urbaneja, M.A.; Bresolin, F.; Przybilla, N.; Gieren, W.; Pietrzyński, G. Quantitative Spectroscopy of 24 A Supergiants in the Sculptor Galaxy NGC 300: Flux-weighted Gravity-Luminosity Relationship, Metallicity, and Metallicity Gradient. *Astrophys. J.* **2008**, *681*, 269–289. [CrossRef] [PubMed]
77. Humphreys, R.M.; Graham, J.A. The M supergiants in NGC 300. *Astron. J.* **1986**, *91*, 522–529. [CrossRef] [PubMed]
78. de Wit, S.; Bonanos, A.Z.; Antoniadis, K.; Zapartas, E.; Ruiz, A.; Britavskiy, N.; Christodoulou, E.; De, K.; Maravelias, G.; Munoz-Sanchez, G.; et al. Investigating episodic mass loss in evolved massive stars: II. Physical properties of red supergiants at subsolar metallicity. *Astron. Astrophys.* **2024**, *689*, 46–68. [CrossRef]
79. Gieren, W.; Pietrzyński, G.; Soszyński, I.; Bresolin, F.; Kudritzki, R.-P.; Storm, J.; Minniti, D. The Araucaria Project: Near-Infrared Photometry of Cepheid Variables in the Sculptor Galaxy NGC 55. *Astrophys. J.* **2008**, *672*, 266–273. [CrossRef]
80. Kudritzki, R.-P.; Castro, N.; Urbaneja, M.A.; Ho, I.-T.; Bresolin, F.; Gieren, W.; Pietrzyński, G.; Przybilla, N. A Spectroscopic Study of Blue Supergiant Stars in the Sculptor Galaxy NGC 55: Chemical Evolution and Distance. *Astrophys. J.* **2016**, *829*, 70–83. [CrossRef]
81. McQuinn, K.B.W.; Boyer, M.L.; Mitchell, M.B.; Skillman, E.D.; Gehrz, R.D.; Groenewegen, M.A.T.; McDonald, I.; Sloan, G.C.; van Loon, J.T.; Whitelock, P.A. DUSTiNGS. III. Distribution of Intermediate-age and Old Stellar Populations in Disks and Outer Extremities of Dwarf Galaxies. *Astrophys. J.* **2017**, *834*, 78–103. [CrossRef]
82. Christodoulou, E.; de Wit, S.; Bonanos, A.Z.; Muñoz-Sanchez, G.; Maravelias, G.; Ruiz, A.; Antoniadis, K.; García-Álvarez, D.; Rubio Díez, M.M. Investigating episodic mass loss in evolved massive stars: IV. Comprehensive analysis of dusty red supergiants in NGC 6822, IC 10, and WLM. *Astron. Astrophys.* **2025**, *704*, 96–117. [CrossRef]
83. Pietrzyński, G.; Gieren, W.; Udalski, A.; Soszyński, I.; Bresolin, F.; Kudritzki, R.-P.; Garcia, A.; Minniti, D.; Mennickent, R.; Szewczyk, O.; et al. The Araucaria Project: The Distance to the Local Group Galaxy WLM from Cepheid Variables Discovered in a Wide-Field Imaging Survey. *Astron. J.* **2007**, *134*, 594–603. [CrossRef]
84. Gieren, W.; Pietrzyński, G.; Szewczyk, O.; Soszyński, I.; Bresolin, F.; Kudritzki, R.-P.; Urbaneja, M.A.; Storm, J.; Minniti, D. The Araucaria Project: The Distance to the Local Group Galaxy WLM from Near-Infrared Photometry of Cepheid Variables. *Astrophys. J.* **2008**, *683*, 611–619. [CrossRef] [PubMed]
85. Bresolin, F.; Pietrzyński, G.; Urbaneja, M.A.; Gieren, W.; Kudritzki, R.-P.; Venn, K.A. The Araucaria Project: VLT Spectra of Blue Supergiants in WLM- Classification and First Abundances. *Astrophys. J.* **2006**, *648*, 1007–1019. [CrossRef]
86. Bonanos, A.Z.; Tramper, F.; de Wit, S.; Christodoulou, E.; Muñoz Sanchez, G.; Antoniadis, K.; Athanasiou, S.; Maravelias, G.; Yang, M.; Zapartas, E. Investigating episodic mass loss in evolved massive stars. I. Spectroscopy of dusty massive stars in ten southern galaxies. *Astron. Astrophys.* **2024**, *686*, 77–142. [CrossRef]
87. Humphreys, R.M. M supergiants and the low metal abundances in the Small Magellanic Cloud. *Astrophys. J.* **1979**, *231*, 384–387. [CrossRef] [PubMed]
88. Massey, P.; Olsen, K.A.G. The Evolution of Massive Stars. I. Red Supergiants in the Magellanic Clouds. *Astron. J.* **2003**, *126*, 2867–2886. [CrossRef]
89. Levesque, E.M.; Massey, P.; Olsen, K.A.G.; Plez, B.; Meynet, G.; Maeder, A. The Effective Temperatures and Physical Properties of Magellanic Cloud Red Supergiants: The Effects of Metallicity. *Astrophys. J.* **2006**, *645*, 1102–1117. [CrossRef]
90. Kelly, P.L.; Diego, J.M.; Rodney, S.; Kaiser, N.; Broadhurst, T.; Zitrin, A.; Treu, T.; Pérez-González, P.G.; Morishita, T.; Jauzac, M.; et al. Extreme magnification of an individual star at redshift 1.5 by a galaxy-cluster lens. *Nat. Astron.* **2018**, *2*, 334–342. [CrossRef]
91. Welch, B.; Coe, D.; Zackrisson, E.; de Mink, S.E.; Ravindranath, S.; Anderson, J.; Brammer, G.; Bradley, L.; Yoon, J.; Kelly, P.; et al. JWST Imaging of Earendel, the Extremely Magnified Star at Redshift z = 6.2. *Astrophys. J. Lett.* **2022**, *940*, L1–L13. [CrossRef]
92. Romagnolo, A.; Belczynski, K.; Klencki, J.; Agrawal, P.; Shenar, T.; Szécsi, D. The role of stellar expansion on the formation of gravitational wave sources. *Mon. Not. R. Astron. Soc.* **2023**, *525*, 706–720. [CrossRef]
93. Diego, J.M.; Li, S.K.; Meena, A.K.; Niemiec, A.; Acebron, A.; Jauzac, M.; Struble, M.F.; Amruth, A.; Broadhurst, T.J.; Cerny, C.; et al. BUFFALO/Flashlights: Constraints on the abundance of lensed supergiant stars in the Spock galaxy at redshift 1. *Astron. Astrophys.* **2024**, *681*, 124–148. [CrossRef]
94. Diego, J.M.; Li, S.K.; Amruth, A.; Meena, A.K.; Broadhurst, T.J.; Kelly, P.L.; Filippenko, A.V.; Williams, L.L.R.; Zitrin, A.; Harris, W.E.; et al. Imaging dark matter at the smallest scales with z $\approx$ 1 lensed stars. *Astron Astrophys.* **2024**, *689*, 167–191. [CrossRef]
95. Diego, J.M.; Adams, N.J.; Willner, S.P.; Harvey, T.; Broadhurst, T.; Cohen, S.H.; Jansen, R.A.; Summers, J.; Windhorst, R.A.; D'Silva, J.C.J.; et al. WST's PEARLS: 119 multiply imaged galaxies behind MACS0416, lensing properties of caustic crossing galaxies, and the relation between halo mass and number of globular clusters at z = 0.4. *Astron. Astrophys.* **2024**, *690*, 114–131. [CrossRef]

96. Schootemeijer, A.; Götberg, Y.; Langer, N.; Bortolini, G.; Hirschauer, A.S.; Patrick, L. A constant upper luminosity limit of cool supergiant stars down to the extremely low metallicity of I Zw 18. *Astron. Astrophys.* **2026**, *707*, 116–132. [CrossRef]
97. Glatzel, W.; Kiriakidis, M. Stability of Massive Stars and the Humphreys/Davidson Limit. *Mon. Not. R. Astron. Soc.* **1993**, *263*, 375–384. [CrossRef]
98. Lovekin, C.C.; Guzik, J.A. Behaviour of Pulsations in Hydrodynamic Models of Massive Stars. In *New Windows on Massive Stars, IAU Symp. 307*; International Astronomical Union; Cambridge University Press: Cambridge, UK, 2015; pp. 176–181. [CrossRef]
99. Davidson, K. Radiation-Driven Stellar Eruptions. *Galaxies* **2020**, *8*, 10. [CrossRef]

Disclaimer/Publisher's Note: The statements, opinions and data contained in all publications are solely those of the individual author(s) and contributor(s) and not of MDPI and/or the editor(s). MDPI and/or the editor(s) disclaim responsibility for any injury to people or property resulting from any ideas, methods, instructions or products referred to in the content.